A Simplified Model of The Floating Caliper Disk Brake With Respect to High Frequency Noise

Thira Jearsiripongkul
Department of Mechanical Engineering, Faculty of Engineering,
Thammasat University, 99 Moo 18 Klong Luang, Pathum Thani 10800,
Tel 66-2-5643001 ext. 3194, Fax 66-2-5643001 ext. 3049,
E-mail: jthira@engr.tu.ac.th

Abstract

High frequency noise from a vehicle is always a concern for any automotive industry looking for passenger comfort. This also holds for the different types of brake noise, which is a source of discomfort both to passengers and passers-by. Intensive research on high frequency noise (between 1-5 kHz) has been carried out. A simplified model of the floating caliper disk brake has been proposed by the author with the aim to predict the onset of high frequency noise. Many possible grounds have been put for the reasons behind this high frequency noise, for example, stick-slip phenomenon, geometry instability, and flutter type instability. Flutter type instability resulting from non-conservative restoring forces is assumed to be the reason behind this particular noise in this model. The stability of the model is studied in term of the friction coefficient between the brake disk and the brake pad. Some parameters, such as braking pressure, damping coefficient of the brake lining, and rotational speed of the brake disk, are also examined and compared with the stability of the system.

Keywords: high frequency noise, disk brake, and instability

1. Introduction

Automotive brakes have experienced substantial changes during the last decades and today disk brakes are standard in passenger cars. In most cars the front brakes are of the disk type. A floating caliper disk brake is the most common type of disk brake and is a highly developed mechanical engineering device.

It is commonly accepted by engineers and scientists working in this field of brake noise, that the high frequency noise in a disk brake is initiated by instability due to the friction forces leading to self-excited vibrations [1]. The reason for the onset of instability has been put forward on different reasons, for example, the change of the friction characteristic with the speed of the contact points [2], the change of the relative orientation of the disk and the brake pads leading to a modification of the friction force [3], and a flutter instability which is found even with a constant friction coefficient [4-6]. It is of course well known, that a negative slope in the friction characteristic leads to instability and self-excitation. But it is also known from laboratory experiments that there may be instability and self-excitation leading to high frequency noise even in the absence of a negative slope of the friction characteristic. The author believes that the flutter instability which may even occur with a constant friction coefficient in most cases is a more realistic cause of high frequency noise.

In this paper, the brake disk has been modeled as a rotating flexible thin plate with a constant rotational speed. The caliper is assumed to remain stationary and the yoke motion is disregarded by considering only the transverse vibrations of the system. The braking forces are directly applied on the brake pads. Both stiffness and damping coefficients of the brake lining and the caliper are to be taken into account and the mass of the brake pad is neglected for all practical purposes. A complex eigenvalue analysis is used to study the stability of the simplified model in terms of the friction coefficients and the effects of various parameters, such as braking pressure, damping coefficient of the brake pad, and rotational speed of the brake disk.

2. A mathematical-mechanical model

2.1 Simplified model analysis

A floating caliper disk brake, shown in Figure 1, consists of a brake disk, brake pads, backing plates, a piston, a caliper, and a yoke. When the brake is actuated, the hydraulic pressure applied to the cylinder of the caliper drives the piston to secure contact between the inner brake pad and the rotating brake disk. Since the hydraulic pressure in the cylinder acts not only on the piston, but also on the base of the cylinder (equal size), as well, the caliper simultaneously slides in the opposite direction to draw the outer brake pad against the rotating brake disk. The braking force is balanced by the yoke.

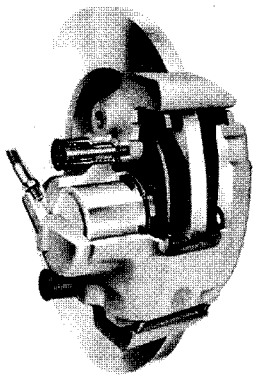

Figure 1. A floating caliper disk brake

In a disk brake model, only the transverse vibration is taken into the account since this motion is important in the frequency range 1-5 kHz confirmed by Dunlap *et al.*[5]. The brake disk is modeled as an annular flexible thin plate (Kirchhoff's plate). It is assumed to be clamped at the inner radius a and free at the outer radius b to rotate about its axis with a constant angular velocity Ω. The system is shown schematically in Figure 2. The brake lining is modeled as a linear elastic spring with stiffness k_p and linear damper with damping coefficient d_p distributed over the sector shown in Figure 2 ($\left[r_p - r_0, r_p + r_0\right] \times \left[-\varphi_0, \varphi_0\right]$) where (r,φ) are the polar coordinates in the inertial frame, r_p is the radius of the center of the brake pad, $2r_0$ is the width of the brake pad in the radial direction, and $2\varphi_0$ is the angle of the brake pad. The caliper is assumed to remain stationary and to connect with the backing plates of the brake pads via linear springs (stiffnesses k_{c1}, k_{c2}) and linear dampers (damping coefficients d_{c1}, d_{c2}) while the braking forces P are directly applied on both brake pads. In this model, the yoke has been neglected due to its motion, which is in the in-plane direction and usually occurs at higher frequency (> 5 kHz).

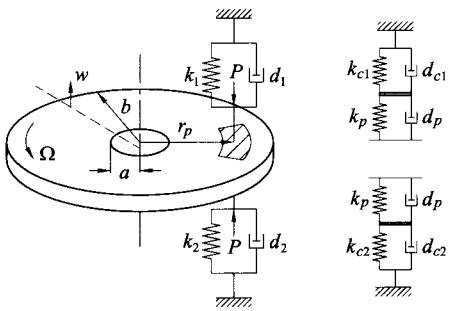

Figure 2. A floating caliper disk brake model

2.2 Equations of motion

The equation of motion for transverse vibrations of the brake disk (Iwan [4]) with the applied force per unit area $\tilde{q}(r,\theta,t)$ is given by:

$$\rho h \frac{\partial^2 \tilde{w}}{\partial t^2} + D\nabla^4 \tilde{w} = \tilde{q}(r,\theta,t) + \frac{1}{r}\frac{\partial}{\partial r}\left(r N_r \frac{\partial \tilde{w}}{\partial r} \right) + \frac{1}{r^2}\frac{\partial}{\partial \theta}\left(N_\theta \frac{\partial \tilde{w}}{\partial \theta} \right) + \frac{1}{r}\frac{\partial}{\partial \theta}\left(N_{r\theta} \frac{\partial \tilde{w}}{\partial r} \right) + \frac{1}{r}\frac{\partial}{\partial r}\left(N_{r\theta} \frac{\partial \tilde{w}}{\partial \theta} \right), \quad (1)$$

where $\tilde{w}(r,\theta,t)$ is the transverse displacement of the brake disk as a function of the body's fixed polar coordinates (material coordinates) r, θ, and of time t, N_r is the radial force per unit length, N_θ is the circumferential force per unit length, and $N_{r\theta}$ is the shear force per unit length. The biharmonic differential operator written in the cylindrical coordinates is:

$$\nabla^4 = \left(\frac{\partial^2}{\partial r^2} + \frac{1}{r}\frac{\partial}{\partial r} + \frac{1}{r^2}\frac{\partial^2}{\partial \theta^2} \right)^2, \quad (2)$$

and the flexural rigidity of a homogeneous disk is:

$$D=\frac{Eh^3}{12\left(1-\nu^2\right)}. \tag{3}$$

The parameters ρ, h, E, and ν are the density, thickness, Young's modulus, and Poisson's ratio of the disk material, respectively.

Due to the rotation of the brake disk and because the radial and tangential displacements induced by this rotation are negligible, it is common to use another set of inertial coordinates r and φ to describe the equations of motion of the brake disk. Based on the aforementioned assumptions, the inertial and material coordinates are related by:

$$\varphi=\theta+\Omega t \quad \forall t\in[0,\infty) \; and \; \theta\in[0,2\pi]. \tag{4}$$

Any function of r, θ, and t can then be written as a different function of r, φ, and t:

$$\tilde{w}(r,\theta,t)=\tilde{w}(r,\varphi-\Omega t,t)=w(r,\varphi,t) \tag{5}$$

Then, the equation of motion in (r,φ) inertial coordinates can be written as:

$$\begin{aligned}\rho h\left(\frac{\partial^2 w}{\partial t^2}+2\Omega\frac{\partial^2 w}{\partial\varphi\partial t}+\Omega^2\frac{\partial^2 w}{\partial\varphi^2}\right)+D\nabla^4 w=q(r,\varphi,t)\\ +\frac{1}{r}\frac{\partial}{\partial r}\left(r\,N_r\frac{\partial w}{\partial r}\right)\\ +\frac{1}{r^2}\frac{\partial}{\partial\varphi}\left(N_\varphi\frac{\partial w}{\partial\varphi}\right)\\ +\frac{1}{r}\frac{\partial}{\partial\varphi}\left(N_{r\varphi}\frac{\partial w}{\partial r}\right)\\ +\frac{1}{r}\frac{\partial}{\partial r}\left(N_{r\varphi}\frac{\partial w}{\partial\varphi}\right).\end{aligned} \tag{6}$$

In this present case the in-plane stresses within the brake disk and centrifugal effect are neglected. These stresses depend on the square of the rotational speed and are small during 'soft' braking. The equation of motion (6) can then be reduced to:

$$\rho h\left(\frac{\partial^2 w}{\partial t^2}+2\Omega\frac{\partial^2 w}{\partial\varphi\partial t}\right)+D\nabla^4 w=q(r,\varphi,t). \tag{7}$$

The transverse displacement of the brake disk in the new coordinate system can be expressed using Galerkin's method:

$$\begin{aligned}w(r,\varphi,t)=\sum_{m=0}^{\infty}\sum_{n=1}^{\infty}R_{m,n}(r)\big[\cos(m\varphi)A_{m,n}(t)\\ +\sin(m\varphi)B_{m,n}(t)\big],\end{aligned} \tag{8}$$

where $R_{m,n}(r)$ are the radial mode shapes of a *stationary* brake disk in terms of the number of the nodal diameter (m) and the number of the nodal circle (n). The generalized coordinates $A_{m,n}(t)$ and $B_{m,n}(t)$ are used to characterize the vibrations of the discretized brake disk. Substituting equation (8) into equation (7) and representing $q(r,\varphi,t)$ in terms of Fourier series, then, comparing the coefficients of $\cos(m\varphi)$ and $\sin(m\varphi)$, leads to:

$$\begin{aligned}\sum_{n=1}^{\infty}\rho h\left(\frac{d^2A_{m,n}}{dt^2}+2m\Omega\frac{dB_{m,n}}{dt}\right)R_{m,n}(r)\\ +DA_{m,n}\tilde{R}_{m,n}(r)=\frac{1}{\pi}\int_0^{2\pi}q(r,\varphi,t)\cos(m\varphi)\,d\varphi\\ \sum_{n=1}^{\infty}\rho h\left(\frac{d^2B_{m,n}}{dt^2}-2m\Omega\frac{dA_{m,n}}{dt}\right)R_{m,n}(r)\\ +DB_{m,n}\tilde{R}_{m,n}(r)=\frac{1}{\pi}\int_0^{2\pi}q(r,\varphi,t)\sin(m\varphi)\,d\varphi\end{aligned} \tag{9}$$

for m = 0, 1, 2, …, ∞ and $\tilde{R}_{m,n}(r)$ is defined as:

$$\tilde{R}_{m,n}(r)=\left(\frac{\partial^2}{\partial r^2}+\frac{1}{r}\frac{\partial}{\partial r}-\frac{m^2}{r^2}\right)^2 R_{m,n}(r) \tag{10}$$

The radial mode shapes $R_{m,n}(r)$ are obtained from the equation of motion for free vibrations of a non-rotating brake disk:

$$\rho h\frac{\partial^2 w}{\partial t^2}+D\nabla^4 w=0. \tag{11}$$

The radial moden shapes, which satisfy equation (11) and the following boundary conditions:

$$\text{(clamped inside)}\quad \begin{aligned}w(a,\varphi,t)&=0,\\ \frac{\partial w}{\partial r}(a,\varphi,t)&=0,\end{aligned} \tag{12}$$

$$\text{(free outside)}\quad \begin{aligned}M_r(b,\varphi,t)&=0,\\ V_r(b,\varphi,t)&=0,\end{aligned} \tag{13}$$

can be represented in terms of the Bessel functions:

$$\begin{aligned}R_{m,n}(r)=C_{1m,n}J_m(\beta_{m,n}r)+C_{2m,n}Y_m(\beta_{m,n}r)\\ +C_{3m,n}I_m(\beta_{m,n}r)\\ +C_{4m,n}K_m(\beta_{m,n}r)\end{aligned} \tag{14}$$

where

$$\omega_{m,n}^2 = \frac{D\beta_{m,n}^4}{\rho h}, \tag{15}$$

is the corresponding natural frequency of mode (m,n). The J_m, Y_m are the m^{th}-order Bessel functions of first and second kind, respectively, the I_m, K_m are the m^{th}-order modified Bessel functions. The constants $C_{1m,n}$, $C_{2m,n}$, $C_{3m,n}$, and $C_{4m,n}$ are found by applying the boundary conditions. These conditions are (12) and (13) while:

$$M_r = -D\left[\frac{\partial^2 w}{\partial r^2} + \nu\left(\frac{1}{r}\frac{\partial w}{\partial r} + \frac{1}{r^2}\frac{\partial^2 w}{\partial \theta^2}\right)\right], \tag{16}$$

$$V_r = -D\left[\frac{\partial}{\partial r}\left(\nabla^2 w\right) + (1-\nu)\frac{1}{r}\frac{\partial}{\partial \varphi}\left(\frac{1}{r}\frac{\partial^2 w}{\partial r \partial \varphi} - \frac{1}{r^2}\frac{\partial w}{\partial \varphi}\right)\right], \tag{17}$$

are the bending moment, and the equivalent shear force (per unit length), respectively.

The following orthogonal condition holds

$$\int_a^b R_{m,n} R_{m,j}\, r\mathrm{d}r = 0 \quad \text{if } n \neq j, \tag{18}$$

one obtains equation (19) as:

$$\rho h\left(\frac{d^2 A_{m,n}}{dt^2} + 2m\Omega\frac{dB_{m,n}}{dt} + \omega_{m,n}^2 A_{m,n}\right) = \frac{1}{\pi}\frac{\int_a^b R_{m,n}\left(\int_0^{2\pi} q(r,\varphi,t)\cos(m\varphi)\mathrm{d}\varphi\right) r\,\mathrm{d}r}{\int_a^b R_{m,n}^2 r\,\mathrm{d}r}$$

$$\rho h\left(\frac{d^2 B_{m,n}}{dt^2} - 2m\Omega\frac{dA_{m,n}}{dt} + \omega_{m,n}^2 B_{m,n}\right) = \frac{1}{\pi}\frac{\int_a^b R_{m,n}\left(\int_0^{2\pi} q(r,\varphi,t)\sin(m\varphi)\mathrm{d}\varphi\right) r\,\mathrm{d}r}{\int_a^b R_{m,n}^2 r\,\mathrm{d}r} \tag{19}$$

where $m = 0, 1, 2, \ldots\infty$ and $j, n = 1, 2, \ldots\infty$ so that j from orthogonal conditions can be simply replaced by n.

The total forces acting on the brake disk are shown in Figure 3 :

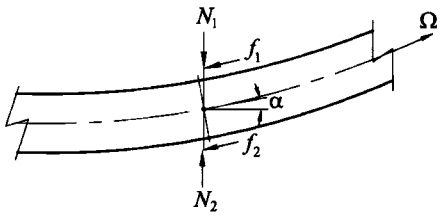

Figure 3. Free body diagram of the brake disk (side view of the brake disk)

and can be described in terms of the force N, including forces from braking, linear springs, and linear dampers, and the friction forces f at the contact between the brake pads and the brake disk with the assumption that the brake pads always remain in contact with the brake disk. The inclination of the brake disk, shown in Figure 3, during vibrations can be approximated as:

$$\alpha \approx \frac{1}{r}\frac{\partial w}{\partial \varphi} \qquad (\alpha \ll 1). \tag{20}$$

The force N on each side of the brake disk can be written in the form of:

$$N_1 = P + k_1 w + d_1\frac{\partial w}{\partial t}, \tag{21}$$

$$N_2 = P - k_1 w - d_2\frac{\partial w}{\partial t}, \tag{22}$$

where k_1, k_2 and d_1, d_2 are the equivalent linear stiffnesses and damping coefficients, respectively, which are modeled by the brake lining and caliper. The friction forces with constant friction coefficient μ is:

$$f_1 + f_2 = \mu\left[2P + (k_1 - k_2)w + (d_1 - d_2)\frac{\partial w}{\partial t}\right], \tag{23}$$

when $\sin\alpha \approx \alpha$ and $\cos\alpha \approx 1$ due to a smallness of inclination. Thus the total applied forces per unit area can be written in form of :

$$q(r,\varphi,t) = -\frac{H(r,\varphi)}{A_L}\left[(k_1 + k_2)w + (d_1 + d_2)\frac{\partial w}{\partial t} + \mu\left(2P + (k_1 - k_2)w + (d_1 - d_2)\frac{\partial w}{\partial t}\right)\frac{1}{r}\frac{\partial w}{\partial \varphi}\right]. \tag{24}$$

Substituting equation (8) into equation (24) and ignoring all nonlinear terms, yields:

$$q(r,\varphi,t)=-\frac{H(r,\varphi)}{A_L}\sum_{k=0}^{\infty}\sum_{l=1}^{\infty}\Big[\Big((k_1+k_2)R_{k,l}(r)B_{k,l}+(d_1+d_2)R_{k,l}(r)\frac{dB_{k,l}}{dt}-\frac{2}{r}\mu k\,PR_{k,l}(r)A_{k,l}\Big)\sin(k\varphi)+\Big((k_1+k_2)R_{k,l}(r)A_{k,l}+(d_1+d_2)R_{k,l}(r)\frac{dA_{k,l}}{dt}+\frac{2}{r}\mu k\,PR_{k,l}(r)B_{k,l}\Big)\cos(k\varphi)\Big] \quad (25)$$

for $k = 0, 1, 2, \ldots \infty$ and $l = 1, 2, \ldots \infty$, where

$$H(r,\varphi)=\begin{cases}1, & \text{if } (r,\varphi)\in D_L\\ 0, & \text{if } (r,\varphi)\notin D_L\end{cases}, \quad (26)$$

D_L is the set representing the contact area between the brake pad and brake disk, and A_L is the net area of D_L. Substituting equation (25) into equation (19), one gets:

$$\rho h\lambda_{mn}^{(7)}\left[\frac{d^2A_{m,n}}{dt^2}+2m\Omega\frac{dB_{m,n}}{dt}+\omega_{m,n}^2A_{m,n}\right]+\sum_{k=0}^{\infty}\sum_{l=1}^{\infty}\lambda_{mn,kl}^{(1)}\frac{dA_{k,l}}{dt}+\sum_{k=0}^{\infty}\sum_{l=1}^{\infty}\lambda_{mn,kl}^{(2)}A_{k,l} \quad (27)$$
$$+\sum_{k=0}^{\infty}\sum_{l=1}^{\infty}\lambda_{mn,kl}^{(3)}B_{k,l}=0$$

$$\rho h\lambda_{mn}^{(7)}\left[\frac{d^2B_{m,n}}{dt^2}-2m\Omega\frac{dA_{m,n}}{dt}+\omega_{m,n}^2B_{m,n}\right]+\sum_{k=0}^{\infty}\sum_{l=1}^{\infty}\lambda_{mn,kl}^{(4)}\frac{dB_{k,l}}{dt}+\sum_{k=0}^{\infty}\sum_{l=1}^{\infty}\lambda_{mn,kl}^{(5)}B_{k,l} \quad (28)$$
$$-\sum_{k=0}^{\infty}\sum_{l=1}^{\infty}\lambda_{mn,kl}^{(6)}A_{k,l}=0$$

where

$$\lambda_{mn,kl}^{(1)}=(d_1+d_2)\int_{r_p-r_0}^{r_p+r_0}R_{m,n}(r)R_{k,l}(r)r\,\mathrm{d}r\int_{-\varphi_0}^{\varphi_0}\cos(m\varphi)\cos(k\varphi)\,\mathrm{d}\varphi \quad (29\text{-a})$$

$$\lambda_{mn,kl}^{(2)}=(k_1+k_2)\int_{r_p-r_0}^{r_p+r_0}R_{m,n}(r)R_{k,l}(r)r\,\mathrm{d}r\int_{-\varphi_0}^{\varphi_0}\cos(m\varphi)\cos(k\varphi)\,\mathrm{d}\varphi \quad (29\text{-b})$$

$$\lambda_{mn,kl}^{(3)}=2\mu kP\int_{r_p-r_0}^{r_p+r_0}R_{m,n}(r)R_{k,l}(r)r\,\mathrm{d}r\int_{-\varphi_0}^{\varphi_0}\cos(m\varphi)\cos(k\varphi)\,\mathrm{d}\varphi \quad (29\text{-c})$$

$$\lambda_{mn,kl}^{(4)}=(d_1+d_2)\int_{r_p-r_0}^{r_p+r_0}R_{m,n}(r)R_{k,l}(r)r\,\mathrm{d}r\int_{-\varphi_0}^{\varphi_0}\sin(m\varphi)\sin(k\varphi)\,\mathrm{d}\varphi \quad (29\text{-d})$$

$$\lambda_{mn,kl}^{(5)}=(k_1+k_2)\int_{r_p-r_0}^{r_p+r_0}R_{m,n}(r)R_{k,l}(r)r\,\mathrm{d}r\int_{-\varphi_0}^{\varphi_0}\sin(m\varphi)\sin(k\varphi)\,\mathrm{d}\varphi \quad (29\text{-e})$$

$$\lambda_{mn,kl}^{(6)}=2\mu kP\int_{r_p-r_0}^{r_p+r_0}R_{m,n}(r)R_{k,l}(r)r\,\mathrm{d}r\int_{-\varphi_0}^{\varphi_0}\sin(m\varphi)\sin(k\varphi)\,\mathrm{d}\varphi \quad (29\text{-f})$$

$$\lambda_{mn}^{(7)}=\pi A_L\int_a^b R_{m,n}^2(r)r\,\mathrm{d}r. \quad (29\text{-g})$$

For example, if two vibrating modes (m,n) and $(m+1,n)$ are considered as the approximate solution (8), the equations of motion (27) and (28) can be written in matrix form as

$$\mathbf{M}\ddot{\mathbf{q}}+(\mathbf{G}+\mathbf{D})\dot{\mathbf{q}}+\mathbf{C}\mathbf{q}=\mathbf{0}, \quad (30)$$

where $\mathbf{q}=\left[A_{m,n},B_{m,n},A_{m+1,n},B_{m+1,n}\right]^T$ and $\mathbf{C}$ is asymmetric due to the friction forces.

3. Numerical results and discussion

The following dimensions and isotropic material properties are used for the brake disk: $a = 90.3$ mm, $b = 152.5$ mm, $\rho = 7{,}050\text{kg/m}^3$, $\nu = 0.21$, $E = 7.74\times10^{10}\,\text{N/m}^2$. The total

thickness of the actual brake disk including the ribs is 26.3 mm, whereas the thickness of the soliddisk in the present analysis is adjusted to 4.56 mm so that the first two natural frequencies of the brake disk match with the equivalent solid disk for the corresponding mode shapes [7].

In the experiment shown in [7], the vibrating modes (7,1) and (8,1) of the equivalent solid disk in the transverse direction were found to be in the frequency range 2,500-2,600 Hz, where high frequency noise usually occurs. The high frequency noise was at 2,554 Hz and measured by a microphone. Subsequently, those two vibrating modes are considered and used to predict the onset of the instability, which is the reason for high frequency noise.

Then the approximate solution (8) can be written as:

$$w(r,\varphi,t) = R_{7,1}\left[\cos(7\varphi)A_{7,1}(t) + \sin(7\varphi)B_{7,1}(t)\right] + R_{8,1}\left[\cos(8\varphi)A_{8,1}(t) + \sin(8\varphi)B_{8,1}(t)\right]. \quad (31)$$

Substituting this approximate solution into equation (19) or using equations (27) and (28) for these particular vibrating modes, one obtains matrices $\mathbf{M}$, $\mathbf{D}$, $\mathbf{G}$, and $\mathbf{C}$ as shown in equation (30) where $\mathbf{q} = \left[A_{7,1}, B_{7,1}, A_{8,1}, B_{8,1}\right]^T$. The stability investigation of the trivial solution will be analyzed with:

$$\begin{aligned} A_{7,1} &= \hat{A}_{7,1}e^{\omega t}, \\ B_{7,1} &= \hat{B}_{7,1}e^{\omega t}, \\ A_{8,1} &= \hat{A}_{8,1}e^{\omega t}, \\ B_{8,1} &= \hat{B}_{8,1}e^{\omega t}. \end{aligned} \quad (32)$$

To study the influence of the friction coefficient μ with the stability of the system, the equivalent stiffnesses k_1 and k_2 are assumed to be equal and the equivalent damping coefficients d_1 and d_2 are assumed to be zero due to simplicity. The behavior of the natural frequencies in considered vibrating modes is studied as a function of the friction coefficient. It is found in each mode that with gradual increment of the friction coefficient the

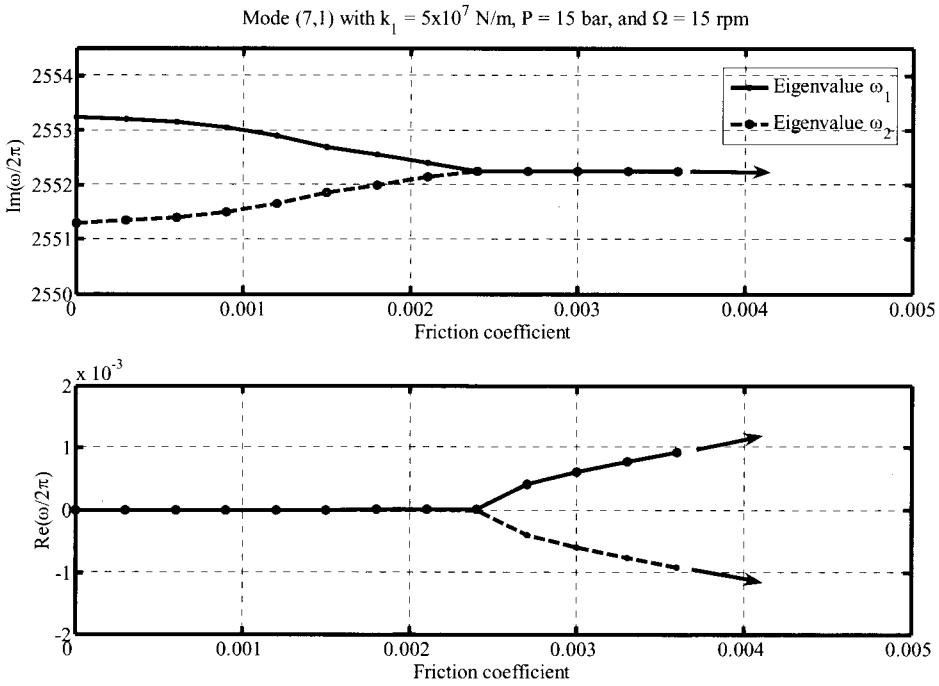

Figure 4. Stability analysis of the vibrating mode (7,1) with the variation of the friction coefficient

asymmetry of stiffness matrix **C** becomes stronger and the natural frequencies become complex at the critical value of the friction coefficient μ_{cr}. This critical value of the friction coefficient defines the onset of the flutter type instability. Subsequently, the gyroscopic term is considered with low rotational speed and the natural frequencies intend to merge as shown in Figure 4 where the onset of the flutter type instability takes place just before the mergence. This plot shows the influence of the friction coefficient on the stability of the system based on eigenvalues. It shows the effects on both real and imaginary parts of the eigenvalues. The critical value of the friction coefficient is about 0.0024 where the real part of the eigenvalues starts splitting, or the imaginary part of the eigenvalues starts merging.

The influence of the braking force P on the stability of the system is shown in Figure 5 in term of the critical value of the friction coefficient while all the other parameters are maintained constant. It shows that the critical value of the friction coefficient tends to decrease with an increment of the braking pressure. The reason is an asymmetry of the stiffness matrix since some off-diagonal elements in this matrix are proportional to the friction force, so that the asymmetry becomes stronger when the braking force increases.

The influences of the linear damping coefficient (d_1 or d_2) and the rotational speed of the brake disk Ω on the stability of the system is also shown in Figure 6 in term of the critical value of the friction coefficient, while all the others parameters are maintained constant as well. The result shows that a linear damping coefficient tends to stabilize the system, where the critical value of the friction coefficient increases, with an increment of the damping coefficient. This is due to the fact that in linear systems a damper is used to improve the stability of the system (higher μ_{cr}). But the higher rotational speed of the brake disk, affecting a gyroscopic term, tends to destabilize the system. The reason behind this is due to the asymmetry in the damping matrix.

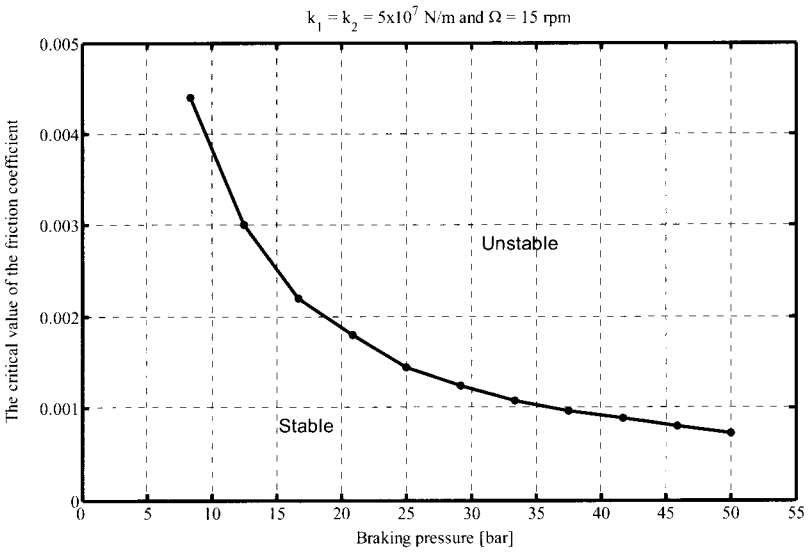

Figure 5. Influence of braking force based on the critical value of the friction coefficient

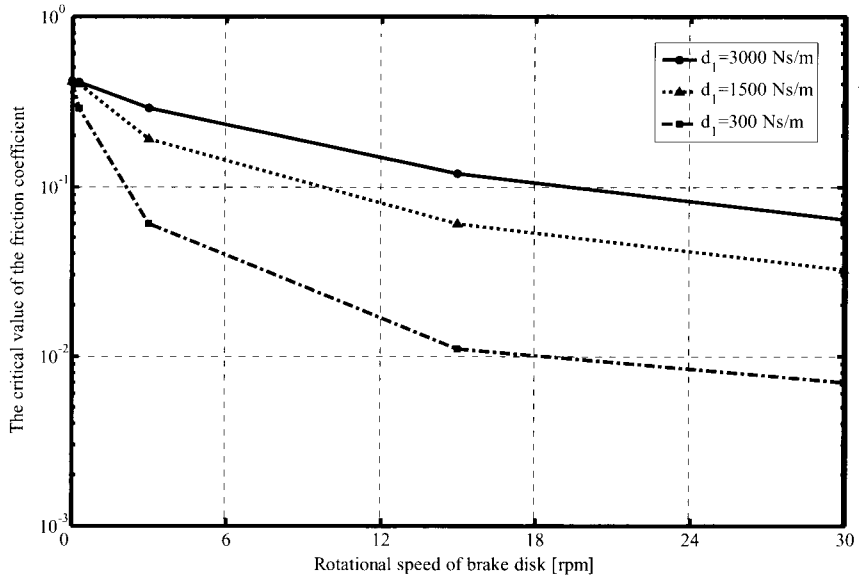

Figure 6. Influence of the damping coefficient and the rotational speed of the brake disk based on the critical value of the friction coefficient

4. Conclusions

A floating caliper disk brake has been modeled and only transverse vibrations of the brake disk are considered. The brake disk is modeled as a Kirchhoff's plate, whereas the brake pads and caliper are assumed to be massless and stationary, respectively. The brake lining is modeled as linear springs and dampers. The friction coefficient between brake disk and brake pads is assumed to be constant.

The stability of the model is analyzed using complex eigenvalue analysis. The undamped model shows flutter type instability or unstable vibrating mode, resulting from the friction force. The braking force and rotational speed of the brake disk tend to destabilize the system, while a damping coefficient of the brake lining always tries to stabilize the system. The author believes that this model can verify the effectiveness of any strategy taken towards controlling the high frequency noise.

5. References

[1] Den Hartog, J.P., Mechanical Vibrations, McGraw-HILL, New York, Fourth Edition, 1956.

[2] Ibrahim, R.A., Friction-induced Vibration, Chatter, Squeal, and Chaos Part II: Dynamics and Modeling, ASME Applied Mechanics Reviews 47:227-259, 1994.

[3] Millner, N., An Analysis of Disc Brake Squeal, SAE Technical Paper Series, 780332, 1978.

[4] Iwan, W.D. and Moeller, T.L., The Stability of a Spinning Elastic Disk with a Transverse Load System, Journal of Applied Mechanics 43(3):485-490, September, 1976.

[5] Dunlap, K.B., Kung, S., and Ballinger, R.S., Complex Eigenvalue Analysis for Reducing Low Frequency Brake Squeal, Technical Report, March, 2000.

[6] Bajaj, A.K., Chowdhary, H.V., and Krousgrill, C.M., An Analytical Approach to Model Disc Brake System for Squeal Prediction, ASME 2001 Design Engineering Technical Conference and Computers and Information in Engineering Conference, September 9-12, 2001.

[7] Breuer, B. and Bill, K. H., Grundlagen, Komponenten, Systeme, und Fahrdynamik: Bremsenhandbuch, ATZMTZ-Fachbuch, Friedr. Vieweg & Sohn Verlag, 2003.